RESEARCH ARTICLES

Control of Axon Branch Dynamics by Correlated Activity in Vivo

Edward S. Ruthazer, Colin J. Akerman, Hollis T. Cline*

To determine how patterned visual activity regulates the development of axonal projections, we collected in vivo time-lapse images of retinal axons from albino *Xenopus* tadpoles in which binocular innervation of the optic tectum was induced. Axons added branch tips with nearly equal probability in all territories, but eliminated them preferentially from territory dominated by the opposite eye. This selective branch elimination was abolished by blockade of *N*-methyl-D-aspartate receptors. These results describe a correlation-based mechanism by which visual experience directly governs axon branch dynamics that contribute to the development of topographic maps.

Sensory maps in the central nervous system result from molecular mechanisms that guide axons to terminate in a crude topographic fashion in their targets (*1*, *2*) and activity-dependent mechanisms that refine this projection to produce precise connectivity (*3*, *4*). These mechanisms have been characterized in detail for the projection from the retina to the tectum, where disruption of neural activity, particularly by inhibition of *N*-methyl-D-aspartate type glutamate receptors (NMDARs), prevents proper development and maintenance of precise connectivity (*5*–*9*).

This lack of precise connectivity after activity blockade is consistent with activity having either a permissive role (in which case activity serves as a switch between a limited set of preprogrammed outcomes) or an instructive role (in which case the precise temporal patterns of firing rather than overall levels of activity carry information that guides the construction of the map). That activity has an instructive rather than permissive effect in refining projections was ultimately shown in studies on fish and frogs in which the normally monocularly innervated optic tectum is surgically induced to become binocularly innervated, resulting in the segregation of inputs into eye-specific territories (*10*–*13*). In this case, the inputs from the two eyes have similar levels of activity and are indistinguishable with respect to molecular guidance cues, but activity is only correlated between neurons from the same eye. Thus, the emergence of the induced ocular dominance bands in these dually innervated tecta indicates that patterned activity can instruct the formation of a novel map (*10*). The maintenance of sensory maps also relies on correlated activity, as indicated by the fact that NMDAR blockers cause desegregation of eye-specific stripes (*14*).

Although the involvement of NMDARs suggests a correlation-based mechanism, little is known about how correlated activity controls the establishment and maintenance of maps. In vivo time-lapse imaging of developing retinal ganglion cell (RGC) axons reveals that branch additions and retractions occur continuously as axons form topographic projections in the optic tectum (*15*–*17*). The rates of dynamic branch rearrangements are sensitive to blockade of presynaptic activity (*18*) and postsynaptic NMDAR activation (*19*). These data suggest that correlated activity leads to map refinement by regulating presynaptic axon branch dynamics. To determine the mechanisms by which activity-dependent cues instructively regulate axon arbor dynamics, we induced dual innervation of the optic tecta of albino *Xenopus laevis* tadpoles and performed time-lapse imaging on retinotectal axons in vivo (*20*).

Binocular tectal innervation. In response to unilateral surgical ablation of the optic tectum at stage 44 (*21*), ipsilateral eye axons crossed the midline through the dorsal posterior commissure and optic chiasm to terminate in the remaining tectal lobe (Fig. 1A). Figure 1B shows a fluorescently labeled RGC axon from the right eye that crossed the posterior commissure and ultimately elaborated within the ipsilateral optic tectum, where it exhibited numerous fine structural rearrangements. One week after surgery (stage 48) the projections from the two eyes were largely overlapping, although eye-spe-

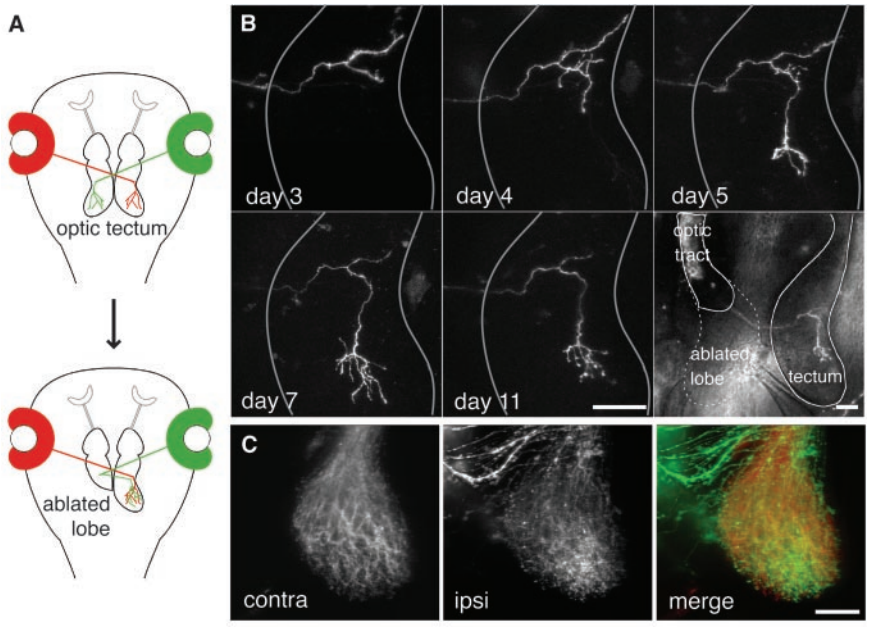

Fig. 1. Surgically induced binocular innervation of the optic tectum. (**A**) The retinotectal projection in tadpoles is normally entirely crossed. Ablation of one tectal lobe at stage 44 causes RGC axons from the ipsilateral eye to innervate the spared tectum within about 1 week. (**B**) Fluorescein isothiocyanate–dextran–labeled RGC axon observed from days 3 to 11 after surgery, as it crossed the dorsal midline to innervate the ipsilateral optic tectum. (Right) Axon superimposed on a low-magnification transmitted-light image of the midbrain. Dashed lines show the position of the ablated tectum. Solid lines outline the intact midbrain regions. (**C**) Bulk labeled contralateral (dil) and ipsilateral eye (diD) projections in a stage 48 tadpole, fixed and labeled 1 week after surgery. Scale bars, 50 μm. Rostral is up in all figures.

Cold Spring Harbor Laboratory, One Bungtown Road, Cold Spring Harbor, NY 11724, USA.

*To whom correspondence should be addressed. E-mail: cline@cshl.edu

cific segregation of inputs was beginning to emerge (Fig. 1C). As others have observed, binocular tectal innervation induced in this manner ultimately produces segregated ocular dominance bands (fig. S1) (*5*, *11*, *12*, *21*).

Branch dynamics underlying segregation. We used this system, in which segregating inputs from the two eyes are still partially overlapping, to characterize the relation between branch dynamics and correlated activity. Correlated activity could influence branch dynamics by (i) inducing addition of axonal branches at sites where activity patterns of inputs are correlated, (ii) stabilizing branches that are coactive with postsynaptic partners, or (iii) selectively eliminating branches whose activity is not correlated with that of their neighbors. Because activity is better correlated among RGCs in the same eye than between RGCs in different eyes, the degree of correlation between an RGC axon and its postsynaptic tectal cell dendrites can be inferred by measuring the relative densities of the afferents from the two eyes to that site in the tectum. Some branches extended in regions mainly innervated by the same eye whereas other branches of the same axon were found in territory dominated by the opposite eye. Therefore, we could directly assess how the degree of afferent correlation affects the addition and elimination of individual axonal branches at a tectal location.

Labeled axons in living tadpoles were imaged at 2-hour intervals for 8 hours (Fig. 2, A to C). There were numerous branch additions and retractions throughout the 8-hour period (Fig. 2C) (*17*, *22*). Dynamic branches were categorized as either added or lost. Added branches were further subdivided into transient and stabilized categories, depending on whether an added branch was subsequently lost or persisted to the end of the 8-hour period (Fig. 2C). At the end of the time-lapse experiment, tadpoles were fixed and the complete ipsilateral and contralateral eye inputs were bulk-labeled with DiD and DiI, respectively. A measure of local ocular dominance was determined for each branch tip by retrospectively matching three-dimensional (3D) computerized reconstructions of the single axon to the confocal z-series stacks of complete ipsilateral and contralateral eye inputs to the tectum (Fig. 2, D and E). Local ocular dominance value was calculated as the logarithm of the ratio of the mean contralateral eye density values to the mean ipsilateral eye density values along the length of the branch tip. This local ocular dominance index is positive in territory where the relative density of contralateral eye afferents is greater than that of ipsilateral eye afferents, and is negative at locations where the ipsilateral eye dominates. Observed values ranged from –1.59 to 1.42, with 90% of values falling between –0.50 and 0.65. The mean local ocular dominance value for all 817 branch tips studied was 0.089 ± 0.012 (*23*), reflecting a slight contralateral bias of inputs in the rewired tecta.

The branch behaviors of an axon are governed by its degree of correlation with other afferents that project to the same sites in the tectum (Figs. 3 and 4). Branch tips of axons originating in the ipsilateral eye (n = 10 animals) (Fig. 3, A and B) showed a significantly lower local ocular dominance value for added branches (0.030 ± 0.037, n = 147 branch tips) than for lost branches (0.147 ± 0.041, n = 109 branch tips) (Fig. 3C, $P < 0.05$, Mann-Whitney U test), suggesting that branches are either preferentially added in same eye territory or lost in territory dominated by the opposite eye.

We distinguished between these two possibilities by sorting branch tips of ipsilateral eye axons on the basis of their local ocular dominance values. All branch tips were divided into three groups of equal size by local ocular dominance score to distinguish branches dominated by ipsilateral, contralateral, and a more equal mixture of both eye inputs. For this analysis, the ipsilateral and contralateral groups were compared, because they represent definitive cases of territory dominated by one eye. A significantly smaller proportion of branches from ipsilateral eye axons was retracted in ipsilateral territory (10.2%) than in territory dominated by the opposite eye (18.1%) (Fig. 3D, $P < 0.05$, χ^2 test). No significant difference in rates of branch addition was found between ipsilateral (21.5%) and contralateral (17.7%) eye territories. Although locations of branch additions were independent of local ocular dominance, the survival of these newly added branches was directly influenced by their local ocular dominance. Only 28.1% of branches added in ipsilateral territory were retracted within the 8-hour experiment, whereas 53.2% of branches added in territory dominated by the contralateral eye were retracted (Fig. 3E, $P < 0.05$, χ^2 test). The local ocular dominance values of stabilized branch tip additions (−0.048 ± 0.048, n = 88 branch tips) were significantly lower (associated with ipsilateral eye territory) than either transiently added (0.147 ± 0.058, n = 59, $P < 0.05$) or lost (0.147 ± 0.041, n = 109) branch tips (Fig. 3C, $P < 0.01$, Kruskal-Wallis with Dunn post-test). These data provide evidence for a correlation-based mechanism of selective branch stabilization or directed elimination, but not for selective branch addition.

To determine whether the above result is a general property of RGC axons in the tectum,

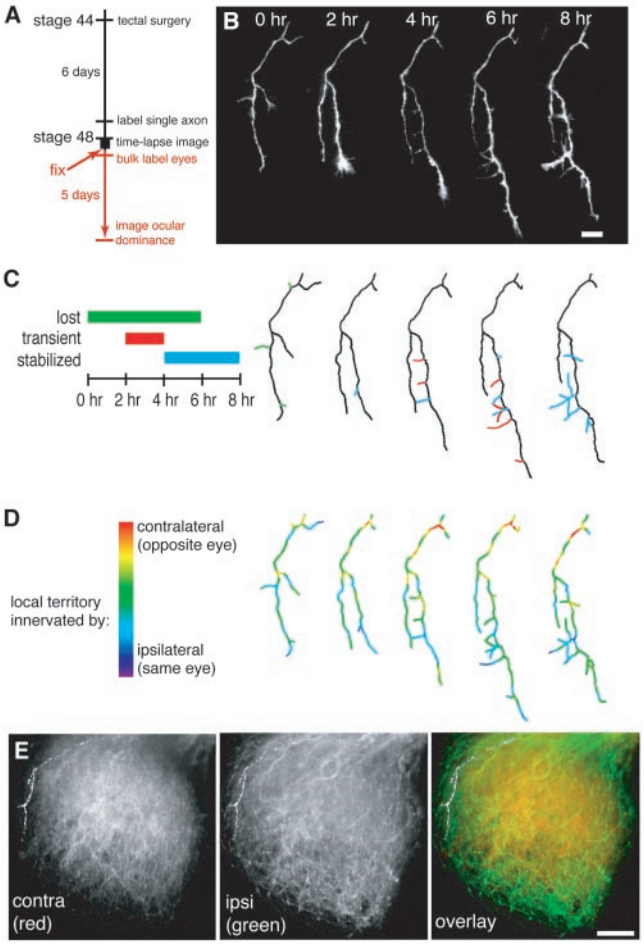

Fig. 2. Experimental methodology. (**A**) Experimental timeline. Postmortem procedures are indicated in red. (**B**) Projected confocal images of a single ipsilateral eye axon at 2-hour intervals in a living tadpole. (**C**) Behaviors of individual branch tips were categorized as lost (green), transient (both added and lost, red), or stabilized (blue) on the basis of reconstructions from time-lapse data. Black indicates the nondynamic portion of the arbor. (**D**) Local ocular dominance of each branch in an arbor was calculated from the relative densities of local ipsilateral and contralateral eye inputs (*20*). (**E**) Retrospective lipophilic bulk labeling of contralateral and ipsilateral retinotectal projections. The axon from (B) is superimposed to show its location in the tectum. Scale bars: (B) 10 μm, (E) 50 μm.

we analyzed branch dynamics from the contralateral eye (*24*). Lost and transient branches were more likely to be located in opposite eye territory. Figure 4, A and B, shows an example of an axon from the contralateral eye in which a rostral tuft of branch tips in ipsilaterally dominated territory retracts and loses branches over 8 hours. Analysis of 13 contralateral eye axons demonstrated that nearly twice as many branches were lost from territory dominated by the ipsilateral (opposite) eye (24.7%) than from contralateral (same) eye territory (14.0%) (Fig. 4C, $P < 0.01$, χ^2 test).

Innervation density modulates dynamics. This experimental system also allowed us to assess the relation between afferent innervation density and branch dynamics. Because new neurons are continually added in the caudomedial proliferative zone of the tectum in frogs, the caudal tectum tends to be relatively sparsely innervated compared with rostral tectum. To examine whether innervation density affects axon branch dynamics, we calculated a local afferent density index for each branch tip from both contralateral and ipsilateral eye axons by summing the contralateral and ipsilateral eye density measurements used to calculate local ocular dominance. This analysis demonstrated that branch tip additions occurred at locations in the tectum that were less densely innervated than sites where nondynamic, persistent branch tips were located (Fig. 4E, $P < 0.01$, Mann-Whitney U test). This effect of innervation density on branch additions also explains the greater fraction of branch additions of contralateral eye axons in ipsilateral (26.5%) than in contralateral (17.6%) territory (Fig. 4C, $P < 0.05$, χ^2 test), because caudal tectum receives more ipsilateral input in these young animals. The subsequent retraction of the contralateral axon branches from ipsilateral territory (Fig. 4D) is consistent with a correlation-based rule for branch dynamics,

Incremental changes in arbor structure lead to segregation into eye-specific zones. It is not possible to observe axon dynamics until complete segregation of eye-specific inputs because the skull thickens and becomes opaque with age. We therefore created a computer simulation to determine whether the rates of branch addition and retraction measured in the time-lapse experiments were sufficient to produce full segregation of inputs from the two eyes into eye-specific patches. Starting with an initially mixed distribution of inputs from the left and right eyes, the empirically derived rates of branch addition and retraction from Figs. 3D and 4C were applied for 180 iterations to simulate 2 months of 8-hour epochs. We imposed a limit in the total allowable input density to prevent branch additions at "saturated" sites, as suggested by the data in Fig. 4E. A clearly segregated set of left and right eye patches emerged in the simulation (Fig. 5). Thus, the rates of branch addition and elimination in 8 hours of time-lapse imaging can ultimately produce segregation of inputs into eye-specific patches. The simulation supports the idea that rapid branch dynamics contribute to the development of an organized retinotectal projection through cumulative modifications in the structure of the axon arbor and its relative position within the target.

Requirement of NMDAR activation. NMDARs are thought to act as detectors of temporal correlation of inputs based on their requirement for both glutamate binding and membrane depolarization to be activated (*5*, *25*). Because the activity-dependent refinement of the retinotectal map in frogs depends on tectal NMDARs (*9*, *14*), we investigated whether NMDAR activity governs axon branch dynamics in contralateral and ipsilateral eye territories by collecting time-lapse images of retinal axons in the presence of the noncompetitive NMDAR antagonist MK-801.

Overnight exposure to MK-801 (10 μM) in the rearing solution blocked all NMDAR-mediated visual responses in tectal neurons, but did not entirely abolish the ability for visual stimuli to evoke activity in the tectum. In untreated control tadpoles, perfusion of the selective NMDAR antagonist D-2-amino-5-phosphonovaleric acid (D-APV, 50 μM) reduced the visually evoked response to 74 ± 7.5% of baseline ($n = 5$), but had no effect in animals that had been exposed overnight to MK-801 (101 ± 16.8% baseline, $n = 5$), suggesting that tectal NMDARs were already fully blocked by overnight exposure to MK-801 (Fig. 6A).

NMDAR blockade completely eliminated any correlations between branch behaviors and local ocular dominance for both contralateral and ipsilateral eye axons (Fig. 6B, $P > 0.05$, Kruskal-Wallis test). The local ocular dominance for all MK-801–treated branch tips (0.11 ± 0.011, $n = 392$) was not significantly different from the value in untreated animals (0.089 ± 0.012, $P > 0.05$, Student's t test). When sorted by local ocular dominance, branch additions (Fig. 6C) and branch retractions (Fig. 6D) occurred with equal frequency in contralateral and ipsilateral territories in tadpoles treated with MK-801 ($P > 0.05$, χ^2 test) (*26*). These data indicate that correlation detection by postsyn-

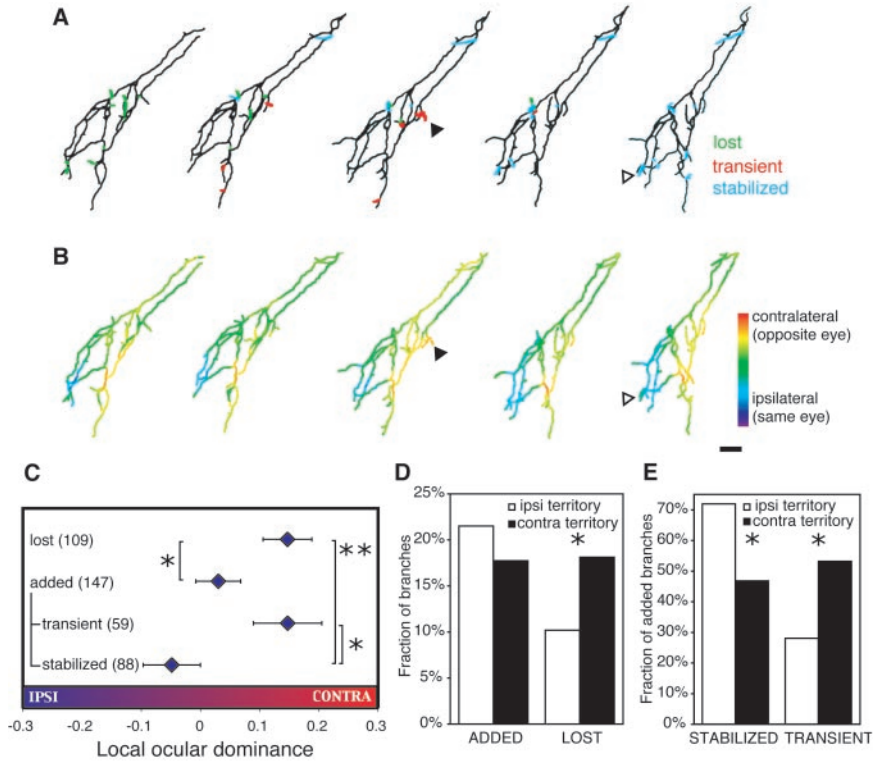

Fig. 3. Ipsilateral eye axons are selectively stabilized in ipsilateral eye territory. (**A**) Flattened 3D reconstruction of an axon from the ipsilateral eye in which branch behaviors are color-coded as in Fig. 2. (**B**) Local ocular dominance profile of axon in (A). Open arrowhead: example of a stabilized branch tip, located in same eye territory; black arrowhead: example of a transient branch, located in opposite eye territory. (**C**) Local ocular dominance values for ipsilateral eye axon branch tips sorted by behavior. Branch tip numbers are in parentheses. (**D**) Fraction of all branch tips in ipsilateral (white) and contralateral (black) eye territories that were added or lost during time-lapse imaging of ipsilateral eye axons. (**E**) Fraction of added branch tips that persisted for the full imaging period (stabilized) or were later observed to retract (transient). *$P < 0.05$, **$P < 0.01$. Scale bar, 10 μm. $n = 408$ branch tips in 10 animals.

aptic NMDARs is required for activity-dependent axon branch tip stabilization or elimination. Interestingly, NMDAR blockade exerts its effects mainly by reducing rates of branch elimination in territory dominated by the opposite eye. This suggests that NMDAR activation contributes to the direct elimination of branches that only weakly drive postsynaptic partners.

Early activity-dependent map refinement. Previous studies in binocularly innervated optic tecta have demonstrated an instructive role for afferent activity and postsynaptic NMDAR activity in maintaining eye-specific segregation during the extended period of larval development and in postmetamorphic froglets (*5*, *9*, *14*), when the retina and tectum both enlarge as a result of cell addition and growth of neuronal processes. The different patterns of growth in the retina and optic tectum require a constant shifting and rescaling of the refined topographic map, which is accomplished by virtue of the continual correlation-based rearrangement of retinotectal connections (*27*, *28*). NMDAR-dependent structural rearrangements of retinal axon arbors can then maintain the precision of the retinotectal connections (*9*, *14*). The data presented here demonstrate that correlated neural activity detected by NMDARs also contributes to the initial formation of refined retinotectal maps. Thus, the mechanisms underlying the topographic refinement of the retinal projection are critical not only for the maintenance of precise connectivity but also for initial map formation.

Mechanisms of structural plasticity in individual axons. We found that correlated activity instructs branch elimination, rather than branch additions, in RGC axons. Previous studies have also shown that NMDAR activation is required for axon branch stabilization (*19*). In normal monocular projections, these mechanisms would serve to sharpen the retinotopic map by stabilizing accurate inputs while eliminating stray branches from topographically inappropriate sites in the eye (*7*, *29*, *30*). The axons in this study added more branches than they retracted overall, resulting in a net addition of new branches in same eye territory over time. By simply comparing two developmental time points, one could easily mistake this observation for evidence of an active mechanism for selective branch addition. However, our time-lapse observations revealed that the accumulation of these new branches was in fact due to branch addition at sites independent of local ocular dominance in conjunction with selective elimination of branches in opposite eye territory.

These observations demonstrate that the classic model of the development of axon projections in which an initially exuberant projection is subsequently pruned by activity-dependent mechanisms (*4*, *31*) does not apply to retinotectal map formation seen in this system. Instead, branch additions and branch pruning are concurrent, so the position of the axon arbor within the target field is gradually adjusted through incremental changes in arbor structure.

The behaviors of individual branch tips from the same axon were regulated independently by local cues in their immediate environments. The NMDAR dependence of local branch elimination suggests that presynaptic axons respond to a retrograde signal generated

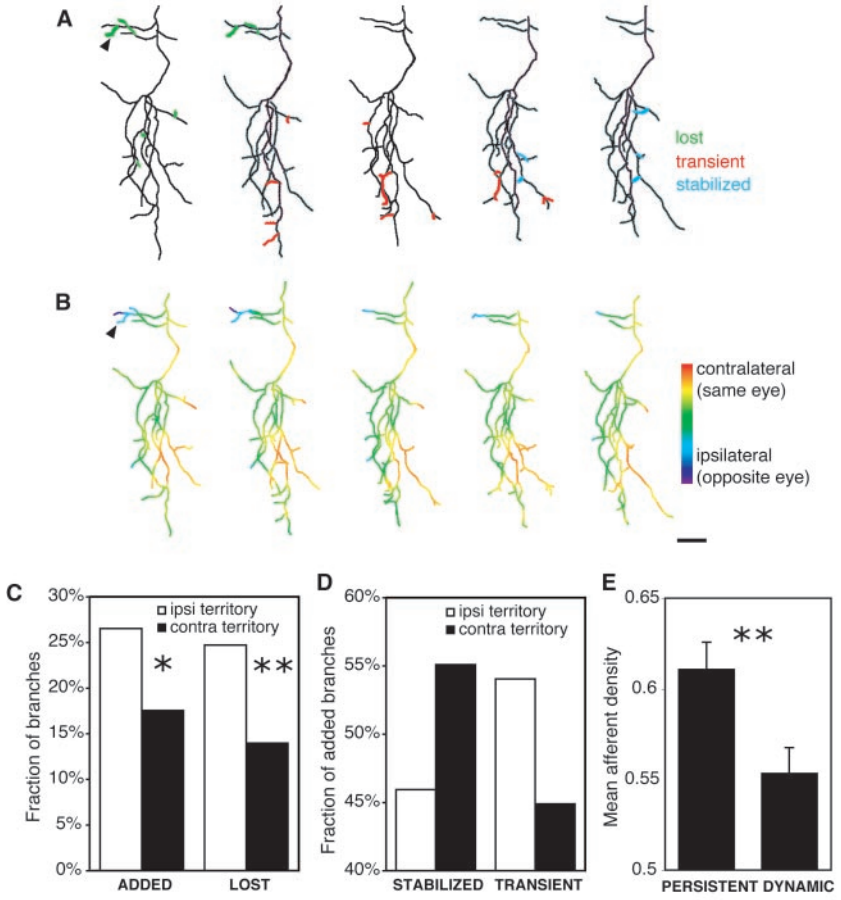

Fig. 4. Contralateral eye axons retract branches preferentially from ipsilateral eye territory. (**A**) Reconstruction of an axon from the contralateral eye in which branch behaviors are color-coded as in Fig. 2. (**B**) Local ocular dominance of axon in (A). Arrowhead indicates an ipsilateral eye–dominated region where branch elimination occurred. (**C**) Fraction of all branch tips in ipsilateral (white) and contralateral (black) eye territories that were added or lost during time-lapse imaging of contralateral eye axons. (**D**) Fraction of added branch tips that persisted for the full imaging period (stabilized) or were later observed to retract (transient). (**E**) Comparison of total local afferent density observed for persistent ($n = 378$) and dynamic ($n = 439$) branch tips. $^*P < 0.05$, $^{**}P < 0.01$. Scale bar, 10 μm. $n = 409$ branch tips in 13 animals in (C) and (D).

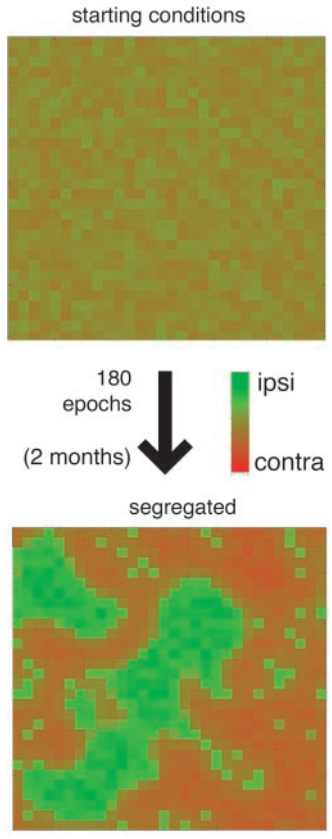

Fig. 5. Simulation of afferent segregation over time based on empirically derived rates of branch addition and retraction (Figs. 3D and 4C). Details of the simulation are given in (*20*).

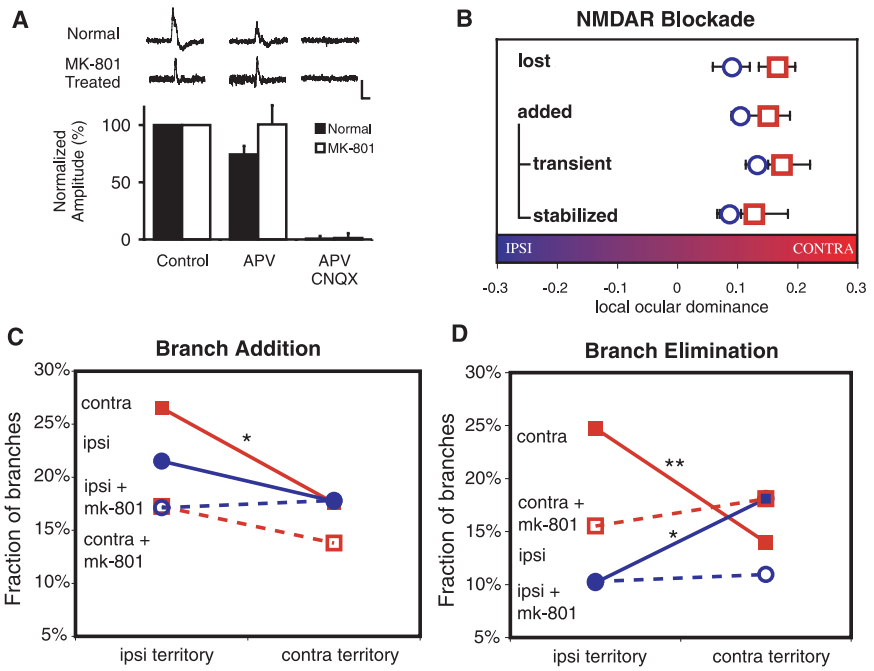

Fig. 6. NMDA receptor blockade abolishes correlations between dynamic branch behaviors and local ocular dominance. (**A**) Effects of acute application of APV (50 μM) or APV plus CNQX (6-cyano-7-nitroquinoxaline-2,3-dione, 20 μM) on visually evoked tectal field potentials in normal stage 48/49 tadpoles ($n = 5$) and animals treated with MK-801 (10 μM) in their rearing solution ($n = 5$). Example traces are the average of 20 trials (scale bars: 0.5 mV and 100 ms). (**B**) Local ocular dominance values sorted by behavior for ipsilateral (circles) and contralateral (squares) eye branch tips in animals treated with MK-801 (10 μM). (**C**) Summary plot of relative rates of branch addition in ipsilateral or contralateral eye–dominated territory. Data for untreated animals (closed symbols) from Figs. 3D and 4C are compared with the results in MK-801–treated tadpoles (open symbols with dashed lines). Axons from the ipsilateral eye are indicated with blue circles and axons from the contralateral eye with red squares. (**D**) Summary plot of relative rates of branch elimination in territory dominated by ipsilateral or contralateral eyes, comparing untreated with MK-801–treated animals. Symbols as in (C). $*P < 0.05$, $**P < 0.01$ (*39*).

at a postsynaptic site where the neural activity patterns of multiple local inputs converge. The spatial extent of these effects may be set by the limited range of a retrograde messenger. The decreased rates of branch elimination in opposite eye territory under NMDAR blockade suggest that poorly correlated activity engages a mechanism of active branch elimination. Similar activity-mediated punitive effects have been described in the developing neuromuscular junction (*32*, *33*) and in the visual cortex of cats during the critical period for ocular dominance plasticity (*34*, *35*).

We also observed that branch additions occur more often in sparsely innervated territory. This provides a possible mechanism by which the correlation-based withdrawal of inputs of one axon could indirectly lead to innervation by other axons. Following branch elimination, the decreased innervation density may promote axon branch addition as seen in the mammalian neuromuscular junction where "synaptic takeover" follows the elimination of competing inputs (*36*). Similarly, in kitten visual cortex, rapid retraction of deprived eye arbors appears to precede the enlargement of axons representing the nondeprived eye in response to monocular deprivation during the critical period (*37*).

Conclusion. Our data describe a mechanism for activity-dependent map refinement through which correlations of patterned neural activity of RGCs actively shape the morphology of their axonal arbors and lead to segregation of afferents into eye-specific territories in the dually innervated tectum. The results indicate that this process occurs by a combination of competitive mechanisms that cause directed branch elimination from inappropriate locations and cooperative mechanisms that lead to selective stabilization of appropriate branches, both of which rely on neural activity through NMDARs. The process of branch addition may be under the control of activity-independent factors (*38*), including a preference for sites of low innervation density.

References and Notes

1. R. W. Sperry, *Proc. Natl. Acad. Sci. U.S.A.* **50**, 703 (1963).
2. J. G. Flanagan, P. Vanderhaeghen, *Annu. Rev. Neurosci.* **21**, 309 (1998).
3. H. T. Cline, *Trends Neurosci.* **14**, 104 (1991).
4. L. C. Katz, C. J. Shatz, *Science* **274**, 1132 (1996).
5. M. Constantine-Paton *et al.*, *Annu. Rev. Neurosci.* **13**, 129 (1990).
6. M. Olson, R. Meyer, *J. Comp. Neurol.* **303**, 412 (1991).
7. D. K. Simon *et al.*, *Proc. Natl. Acad. Sci. U.S.A.* **89**, 10593 (1992).
8. L. Gnuegge *et al.*, *J. Neurosci.* **21**, 3542 (2001).
9. H. T. Cline, M. Constantine-Paton, *Neuron* **3**, 413 (1989).
10. M. Constantine-Paton, M. I. Law, *Science* **202**, 639 (1978).
11. R. L. Meyer, *Science* **218**, 589 (1982).
12. V. C. Boss, J. T. Schmidt, *J. Neurosci.* **4**, 2891 (1984).
13. T. Reh, M. Constantine-Paton, *J. Neurosci.* **5**, 1132 (1985).
14. H. T. Cline *et al.*, *Proc. Natl. Acad. Sci. U.S.A.* **84**, 4342 (1987).
15. R. J. Kaethner, C. A. Stuermer, *J. Neurosci.* **12**, 3257 (1992).
16. N. A. O'Rourke *et al.*, *Neuron* **12**, 921 (1994).
17. S. Witte *et al.*, *J. Neurobiol.* **31**, 219 (1996).
18. S. Cohen-Cory, *J. Neurosci.* **19**, 9996 (1999).
19. I. Rajan *et al.*, *J. Neurobiol.* **38**, 357 (1999).
20. Materials and methods are available as supporting material on *Science* Online.
21. C. Straznicky, J. Glastonbury, *J. Embryol. Exp. Morphol.* **50**, 111 (1979).
22. Previous data show that a 2-hour imaging interval underestimates the total number of rapid branch rearrangements, but it greatly reduces the risk of phototoxicity. It also ensured that animals received considerable natural visual experience during the intervals between image collection. Imaging and full recovery from anesthesia require about 15 min. Thus, the tadpoles spent at least 85% of the experimental period swimming and experiencing natural vision.
23. All values are presented as the mean ± SEM.
24. This analysis also allowed us to exclude the possibility that the results seen in ipsilateral axons may have been due to the contribution of a population of regenerating ipsilateral axons that were potentially severed during tectal surgery.
25. G. S. Stent, *Proc. Natl. Acad. Sci. U.S.A.* **70**, 997 (1973).
26. The overall contralateral bias of inputs is reflected in the mean local ocular dominance of MK-801–treated branch tips (Fig. 6B), but does not severely affect the comparison between branch behaviors in ipsilaterally dominated and contralaterally dominated territories (Fig. 6, C and D)
27. R. M. Gaze *et al.*, *J. Embryol. Exp. Morphol.* **53**, 103 (1979).
28. T. Reh, M. Constantine-Paton, *J. Neurosci.* **4**, 442 (1984).
29. J. T. Schmidt *et al.*, *J. Neurobiol.* **42**, 303 (2000).
30. A. J. Dawson, R. L. Meyer, *J. Comp. Neurol.* **434**, 40 (2001).
31. D. H. Hubel, T. N. Wiesel, *Proc. R. Soc. London Ser. B* **198**, 1 (1977).
32. R. J. Balice-Gordon, J. W. Lichtman, *Nature* **372**, 519 (1994).
33. J. W. Lichtman, H. Colman, *Neuron* **25**, 269 (2000).
34. Y. Hata, M. P. Stryker, *Science* **265**, 1732 (1994).
35. C. D. Rittenhouse *et al.*, *Nature* **397**, 347 (1999).
36. M. K. Walsh, J. W. Lichtman, *Neuron* **37**, 67 (2003).
37. A. Antonini, M. P. Stryker, *J. Comp. Neurol.* **369**, 64 (1996).
38. P. A. Yates *et al.*, *J. Neurosci.* **21**, 8548 (2001).
39. $n = 409$ contra untreated, 408 ipsi untreated, 168 contra MK-801–treated, 224 ipsi MK-801–treated branch tips. n (lost, added, transient, stabilized) for contra axons = (59, 49, 25, 24) in five animals, n for ipsi axons = (58, 87, 34, 53) in five animals.

40. Supported by the NIH (E.S.R., H.T.C.), Helen Hoffritz Foundation (H.T.C.), and a Wellcome Trust International Fellowship (C.J.A.). We thank S. Kaell and J. Pinezich of Advanced Acoustic Concepts for help with the computer simulation; K. Svoboda, B. Burbach, and P. O'Brien for guidance in constructing the two-photon microscope; M. Stryker for comments on the manuscript; and the members of the Cline laboratory for comments on the manuscript and constructive discussions.

Supporting Online Material
www.sciencemag.org/cgi/content/full/301/5629/66/DC1
Materials and Methods
Fig. S1
Reference

21 January 2003; accepted 6 May 2003

Supporting Online Material

Materials and Methods

All experimental protocols were approved by the Cold Spring Harbor Laboratory Animal Care and Use Committee and complied with the guidelines established in the Public Health Service Guide for the Care and Use of Laboratory Animals.

Tectal surgery to induce binocular innervation Stage 44 tadpoles were briefly anesthetized in 0.01% MS-222 (Sigma) dissolved in Steinberg's solution. Using the tip of a 30ga syringe needle, inserted through the skin at the midline between the two tectal lobes, one tectal lobe was severed from the thalamus and underlying tegmentum. A glass micropipette with a 50µm tip was inserted alongside the needle and suction applied to extract the tectum unilaterally.

Labeling of individual RGC axons Stage 48 tadpoles were anesthetized in 0.01% MS-222 solution and placed on an electrically grounded moist kimwipe. The tip of a fine glass micropipette filled with a solution of either 0.02% 1,1'-dioctadecyl-3,3,3',3'-tetramethylindocarbocyanine perchlorate (DiI, Molecular Probes) in ethanol or 5%10KD molecular weight fluorescein-conjugated dextran (FITC-dextran, Molecular Probes) in 0.1M phosphate buffered saline was inserted into the RGC layer of the eye. For initial experiments using confocal microscopy, DiI was used to label axons. FITC-dextran was found to be superior for two-photon imaging, and was used in all subsequent experiments. Current was passed until a small amount of dye could be seen deposited in the retina. Animals were screened under epifluorescence for successful labeling after 24 hr transport time.

Time lapse imaging Tadpoles with single or a few discrete labeled RGC axons were anesthetized in 0.01% MS-222 solution and placed in a Sylgard chamber which immobilized animals while a single z-series (1.5µm steps) was collected using either a Noran Oz confocal microscope with a Nikon 40x oil immersion objective(N.A. 1.2) or a custom-built two-photon laser-scanning microscope with an Olympus 40x water immersion lens (N.A. 0.8). Animals were placed in a bath containing fresh Steinberg's solution during the interval between imaging sessions. In the case of drug treatment, 10mM MK-801 (RBI) stock solution was applied to the rearing solution to achieve a 10µM final concentration 12 hr prior to imaging. During the interval between imaging sessions, animals were maintained in fresh MK-801 solution.

Bulk labeling of the retinotectal projections from each eye After imaging, animals were fixed overnight in 4% paraformaldehyde in phosphate buffer. 0.2% solutions of diI and 1,1'-dioctadecyl-3,3,3',3'- tetramethylindodicarbocyanine perchlorate (diD) in ethanol were intraocularly injected using a Picospritzer II (General Valve) to completely fill each eye. After about one week transport time at room temperature, confocal z-series of the bulk label patterns from the two eyes were collected. Very few RGC axons failed to be labeled by this technique, as demonstrated by test injections in which both dyes were

injected independently into the same eye resulting in identical labeling patterns. In postmetamorphic frogs the complete retinotectal projection was labeled by severing the optic nerve under MS-222 anesthesia and applying a piece of gelfoam saturated with FITC-dextran or Texas Red-dextran (10K, Molecular Probes). After 48 hr transport, frogs were deeply anesthetized in MS-222 and fixed by transcardial perfusion of 4% paraformaldehyde in 0.1M phosphate buffer.

Three-dimensional alignment of time lapse and bulk label images Three-dimensional axon reconstructions were created for each time point using Object-Image software and custom macros (http://www.cshl.org/labs/cline/morphometry.html) (*1*). Analysis was limited to non-lamellar processes longer than 2µm. Reconstructions were aligned to the FITC channel of triple-labeled FITC(single axon)/DiI(contralateral eye)/DiD(ipsilateral eye) z-series confocal stacks. To integrate input density in the vicinity of the axon, diI and diD images were Gaussian smoothed with a 2.5µm half-width at half-height filter prior to alignment. Pixel brightness values were then normalized to derive contralateral eye density and ipsilateral eye density maps for each animal by setting the brightest point in each channel to a density value of 1 and the background to 0. For each branch tip, these normalized contralateral eye density values and ipsilateral eye density values were each averaged along its length to calculate mean contralateral density and mean ipsilateral density respectively. A single *local ocular dominance* value was calculated for each branch tip by taking the log of its mean contralateral eye density divided by its mean ipsilateral eye density. Local ocular dominance values for all branch tips were normally distributed as assessed by a Kolmogorov-Smirnov test for normality ($P>0.05$).

Recording Visually Evoked Field Recordings Stage 48/49 tadpoles were deeply anaesthetized in MS222, transferred to extracellular saline (115 mM NaCl, 4 mM KCl, 3 mM $CaCl_2$, 3 mM $MgCl_2$, 5 mM HEPES, 10 µM Glycine, 10 mM Glucose [pH 7.2]) and stabilized on a piece of Sylgard with dissecting pins. To record the visually evoked field potentials, the skin overlying the tecta was removed and an extracellular recording electrode, consisting of a glass micropipette filled with extracellular saline, was placed in the optic tectum contralateral to the eye that was stimulated. Recordings were performed with an Axopatch-200B amplifier in current clamp mode and digitized using pClamp-8 software and a Digidata-1322A A/D-board (Axon Instruments). Visual stimuli were whole field flashes of diffuse light from a computer-controlled LED (λd = 574 nm; Allied Electronics). The LED was positioned 25mm from the eye and light flashes were presented as 0.1 Hz square wave cycles. At these stages, responses to decreases in luminance (off responses) are greater than responses to increases in luminance. Thus the visually evoked field potential was measured using a 5ms window placed at the peak of the off response.

Computer simulation based on empirical data The simulation consisted of one 30-by-30 pixel layer (tectum) with variable ipsi and contra input strengths. Adjustments to input strengths were calculated for each iteration by multiplying instantaneous strength by the probabilities graphed in Figs. 6 C and D. Three simple rules were applied for180 iterations: (1) Local ocular dominance was determined pixel-by-pixel for each iteration

based on which eye had the greater input strength at that pixel during that iteration. (2) Whenever the total input strength to a pixel exceed an arbitrary limit of 2, input addition was restricted, but input elimination could continue. (3) To emulate the 2D structure of arbors, changes in input strengths at any pixel also caused similar modifications to the neighboring 8 pixels at a strength of 1/8 that at the central pixel. The starting input strengths were randomly chosen within the following ranges: ipsi (0 to 0.5), contra (0.1 to 0.85). A slight contralateral bias was applied to mimic conditions experienced by ipsilateral eye axons invading the contralaterally dominated tectum. The simulation was implemented using MATLAB software.

Reference

1. E. S. Ruthazer, H. T. Cline, *Real-Time Imaging* **8**, 175 (2002).